Supplementary Materials

Little change in Palmer Drought Severity Index across global land under warming in climate projections

Yuting Yang[1,7], Shulei Zhang[1,2,7], Michael L. Roderick[3,4], Tim R. McVicar[4,5], Dawen Yang[1], Wenbin Liu[6], Xiaoyan Li[2]

1State Key Laboratory of Hydroscience and Engineering, Department of Hydraulic Engineering, Tsinghua University, Beijing, China

2State Key Laboratory of Earth Surface Process and Resource Ecology, School of Natural Resources, Faculty of Geographical Science, Beijing Normal University, Beijing, China

3Research School of Earth Sciences, Australian National University, Canberra, ACT, Australia

4Australian Research Council Centre of Excellence for Climate Extremes, Canberra, ACT, Australia

5CSIRO Land and Water, Canberra, ACT, Australia

6Key Laboratory of Water Cycle and Related Land Surface Processes, Institute of Geographic Sciences and Natural Resources Research, Chinese Academy of Sciences, Beijing, China

7Equal contribution.

Corresponding Author: Yuting Yang (yuting_yang@tsinghua.edu.cn)

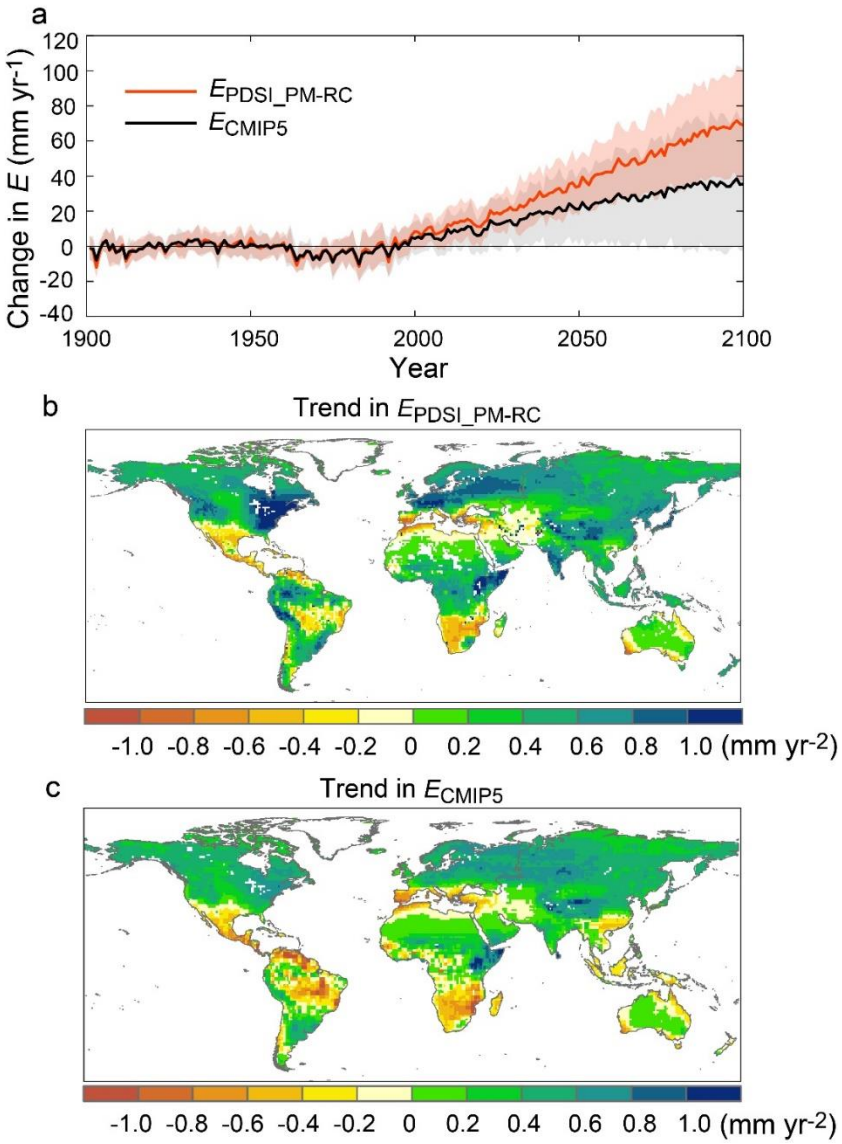

Supplementary Figure S1. Evapotranspiration estimated using the standard PDSI model forced with reference crop E_P ($E_{PDSI\_PM\text{-}RC}$) compared with the direct output from the CMIP5 models (E_{CMIP5}). **a**, Changes in annual mean $E_{PDSI\_PM\text{-}RC}$ and E_{CMIP5} relative to the 1901-1960 baseline. The solid curves represent the ensemble mean of 16 CMIP5 models and the shaded areas are plus/minor one standard deviation among models. **b**, Spatial distribution of trend in annual $E_{PDSI\_PM\text{-}RC}$ over 1901-2100. **c**, Spatial distribution of trend in annual E_{CMIP5} over 1901-2100.

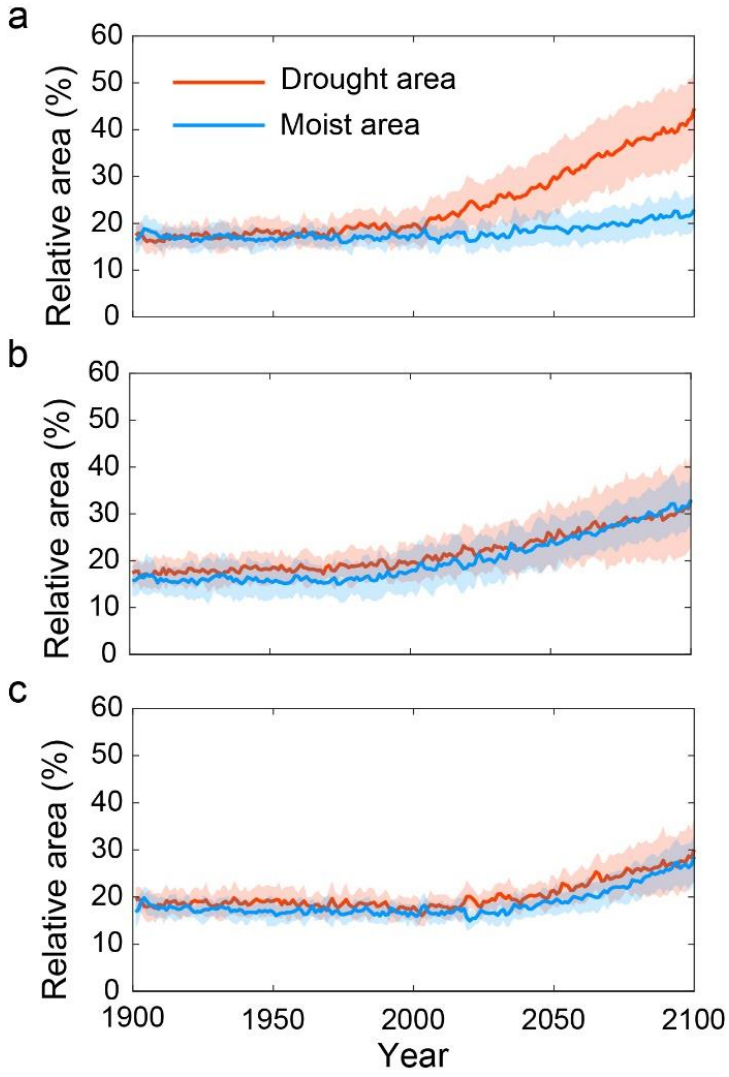

Supplementary Figure S2 Global average time series of fractional land area experiencing drought/moist conditions. a-c, Global average time series of land area experiencing drought (PDSI < -2.0, red) and moist (PDSI > 2.0, blue) conditions for (a) PDSI_PM-RC, (b) PDSI_CMIP5 and (c) PDSI_PM[CO_2], respectively. The solid curve represents the ensemble mean of 16 CMIP5 models and the shading represents plus/minus one standard deviation among models.

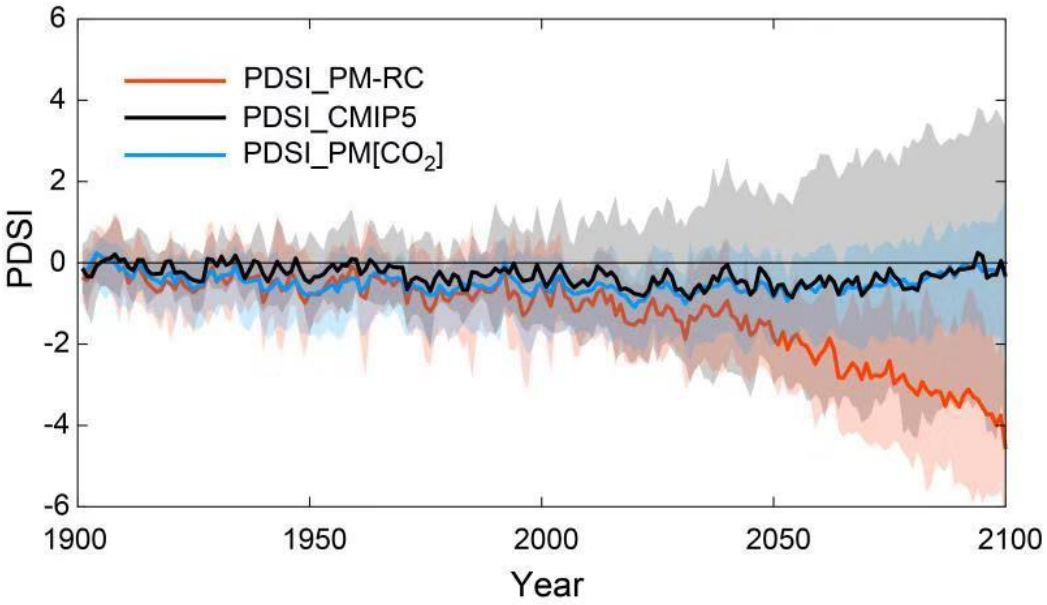

Supplementary Figure S3 Time series of the three PDSIs at the global scale. Here the PDSI is calculated using the global averaged forcing variables.

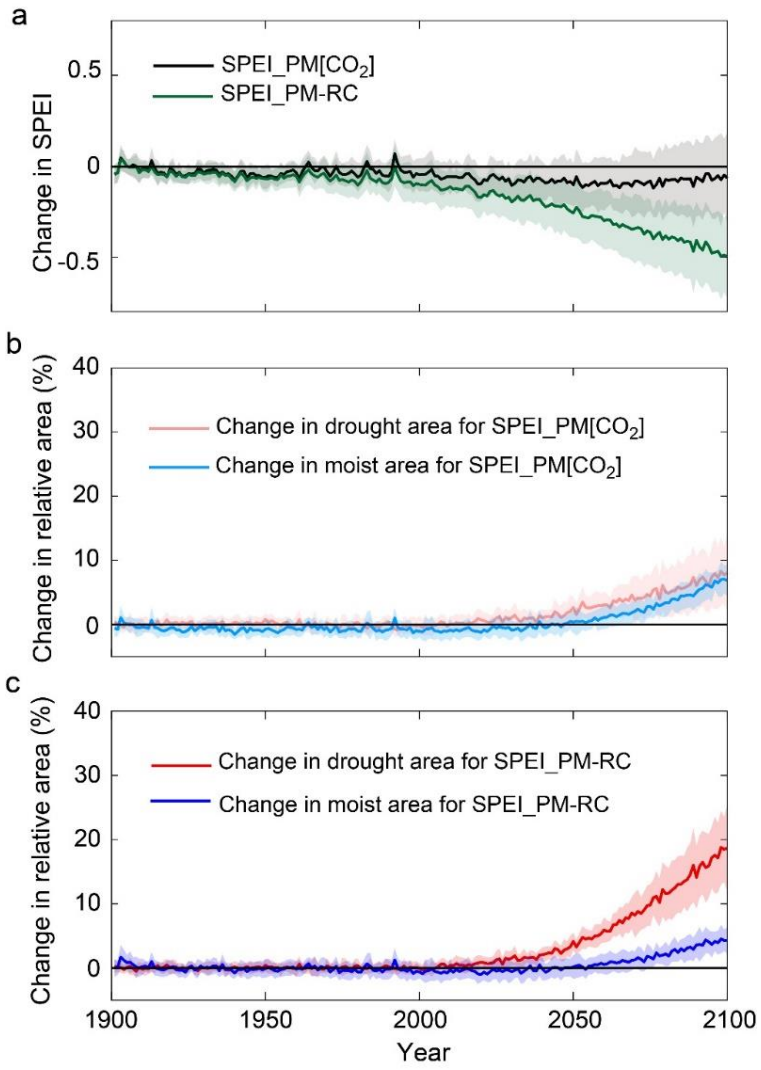

Supplementary Figure S4. Changes in global mean Standardised Precipitation-Evapotranspiration Index (SPEI) and area in drought/moist relative to the 1901-1960 baseline. **a**, SPEI with E_P calculated from the reference crop Penman-Monteith E_P (SPEI_PM-RC; green line) and SPEI with E_P calculated from the modified Penman-Monteith model with CO_2 adjustment (SPEI_PM[CO_2]; black line). **b**, Changes in drought (SPEI < -1.5) and moist (SPEI > 1.5) areas relative to the 1901-1960 baseline detected by SPEI_PM[CO_2]. **c**, Changes in drought (SPEI < -1.5) and moist (SPEI > 1.5) areas relative to the 1901-1960 baseline detected by SPEI_PM-RC. The solid curves represent the ensemble mean of 16 CMIP5 models and the shaded areas are plus/minor one standard deviation among models.

Table S1. The 16 CMIP5 models used in this study.

Model name	Nation	Modeling Center	Reference
bcc-csm1-1	China	Beijing Climate Center, China Meteorological Administration	Wu et al. [2012]
bcc-csm1-1-m	China	Beijing Climate Center, China Meteorological Administration	Wu et al. [2012]
BNU-ESM	China	Beijing Normal University	Wei et al. [2012]
CNRM-CM5	France	Centre National de Recherches Météorologiques	Voldoire et al., [2013]
GFDL-ESM2G	USA	NOAA Geophysical Fluid Dynamics Laboratory	Dunne et al. [2012]
GFDL-ESM2M	USA	NOAA Geophysical Fluid Dynamics Laboratory	Dunne et al. [2012]
GISS-E2-H	USA	NASA Goddard Institute for Space Studies	Schmidt et al. [2014]
GISS-E2-R	USA	NASA Goddard Institute for Space Studies	Schmidt et al. [2014]
IPSL-CM5A-LR	France	Institute Pierre-Simon Laplace	Hourdin et al. [2013]
IPSL-CM5A-MR	France	Institute Pierre-Simon Laplace	Hourdin et al. [2013]
IPSL-CM5B-LR	France	Institute Pierre-Simon Laplace	Hourdin et al. [2013]
MIROC5	Japan	National Institute for Environmental Studies, The University of Tokyo	Watanabe et al. [2011]
MIROC-ESM	Japan	National Institute for Environmental Studies, The University of Tokyo	Watanabe et al. [2011]
MIROC-ESM-CHEM	Japan	National Institute for Environmental Studies, The University of Tokyo	Watanabe et al. [2011]
NorESM1-M	Norway	Norwegian Climate Centre	Bentsen et al. [2013]
NorESM1-ME	Norway	Norwegian Climate Centre	Bentsen et al. [2013]

References in Supplementary Table S1

Bentsen, M. et al: The Norwegian Earth System Model, NorESM1-M – Part 1: Description and basic evaluation of the physical climate, Geosci. Model Dev., 6, 687-720, 2013.

Dunne, J. P. et al: GFDL's ESM2 Global Coupled Climate–Carbon Earth System Models. Part I: Physical Formulation and Baseline Simulation Characteristics, J.

Clim., 25, 6646-6665, 2012.

Hourdin, F., et al: Impact of the LMDZ atmospheric grid configuration on the climate and sensitivity of the IPSL-CM5A coupled model, Clim. Dyn., 40, 2167-2192, 2013.

Schmidt, G. A., et al: Configuration and assessment of the GISS ModelE2 contributions to the CMIP5 archive, J. Adv. Model. Earth Sy., 6, 141-184, 2014.

Voldoire, A., et al: The CNRM-CM5.1 global climate model: description and basic evaluation, Clim. Dyn., 40, 2091-2121, 2014.

Watanabe, S., et al: MIROC-ESM 2010: model description and basic results of CMIP5-20c3m experiments, Geosci. Model Dev., 4, 845-872, 2011.

Wei, T., et al: Developed and developing world responsibilities for historical climate change and CO_2 mitigation. Proc. Natl. Acad. Sci. U.S.A., 109, 12911-12915, 2012.

Wu, T.: A mass-flux cumulus parameterization scheme for large-scale models: description and test with observations, Clim. Dyn., 38, 725-744, 2012.